

# Analytical and Numerical Simulation of Multipactor within a Helical Resonant Filter

David A. Constable, Paul McElhinney, Chris Lingwood, Graeme Burt  
Engineering Department, Lancaster University  
Lancaster, United Kingdom  
d.constable@lancaster.ac.uk

Giuseppe Salza, George Goussetis  
Heriot-Watt University  
Edinburgh, United Kingdom

*Abstract* — Multipactor analysis of a helical resonant filter has been performed using CST Particle Studio and analytically using a 1-D particle tracking code, based on the Runge-Kutta-Nystrom method. A comparison of results is presented.

*Keywords*—multipactor; helical resonant filter; CST Particle Studio; Runge-Kutta-Nystrom method.

## I. INTRODUCTION

Helical resonator filters [1-2] are often used in space-borne communications, due to their relatively compact size and high Q factor capabilities. However, their power handling capabilities are limited, which reduces their lifetime, and, in extreme cases, the lifetime of their satellite [3]. In such a situation, the runaway production of secondary electrons, known as multipactor [4], degrades the electrical performance of the device. The secondary emission yield (SEY) of the material the system is made of, along with the geometry, frequency of operation and RF power all play a role in the onset of multipactor. Therefore, it is of critical importance to be able to model, predict and potentially limit its presence within a system, as has previously been done for simple geometries [5].

One such helical resonant filter, with a passband at 300 MHz, has been the subject of an investigation with the Particle-in-Cell code, CST Particle Studio, to observe the conditions under which multipactor occurs. Similar structures have received previous experimental and analytic consideration [6]. A cut-plane view of the geometry examined is shown in Figure 1; here, the two internal helices are connected to co-axial lines, which provide the RF to the system.

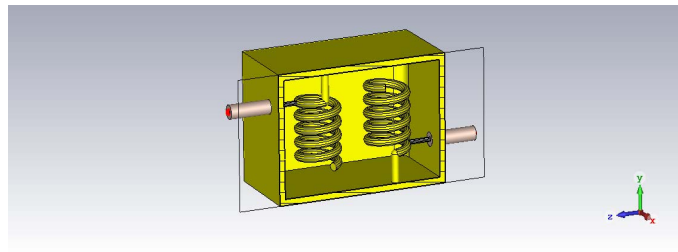


Figure 1 – Investigated geometry, as modelled in CST Particle Studio.

In addition, a 1-D particle tracking code has been developed, which employs the Runge-Kutta-Nystrom [7] method. This code allows for the rapid calculation of particle trajectories and impact energies, as a function of both electric field magnitude and phase. A brief description and overview of some results will be presented.

## II. NUMERICAL AND ANALYTICAL SIMULATIONS

Prior to consideration of particles, the electric and magnetic fields corresponding to operation of the filter at 300 MHz are exported from CST Microwave Studio. This allows them to be imported into a subsequent CST Particle Studio calculation, within which the power can be varied. The electric field maxima occurs at the end of each helix, as shown in Figure 2. In this area, the distance between the edge of the helix and the bounding box is its smallest. This area is therefore referred to as region of critical multipactor – i.e. where multipactor is most likely to occur. In this region, the field falls off with a  $1/r$  dependence.

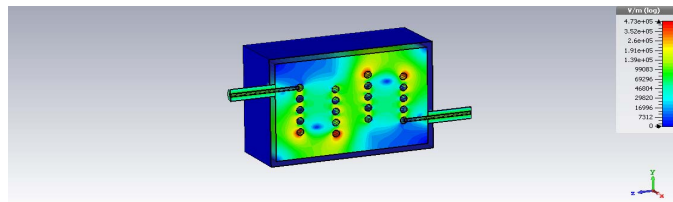
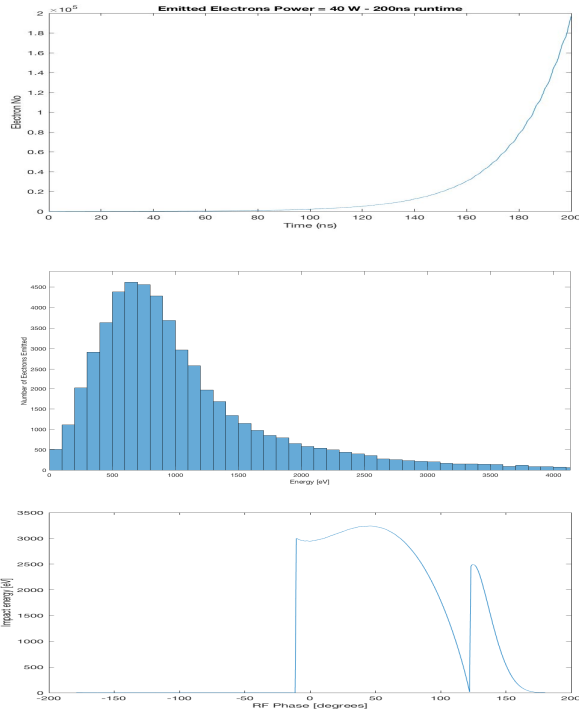


Figure 2 – Example of the absolute electric field profile within the simulated geometry, from CST Particle Studio.

For an initial population of 10 electrons within the volume, their response to the fields is observed in CST Particle Studio. Each of the simulations are run for a simulation time of 200 ns – this allows the rapid growth of electrons to be observed, without the physical run time of the simulation becoming large. For the simulation described, we consider that the helix and wall are made of silver, which has a peak SEY of 1.2 at an energy of 300 eV, for impact angle of 0 degrees. Figure 3 shows the number of electrons as a function of time. Here, the exponential growth in the number of electrons is clear, with approximately 200,000 particles existing after 200 ns. The average impact energy per particle at each time-step can be calculated from the CST Particle Studio results. Consideration of this over the entire simulation gives an

average SEY of  $\sim 1.2$ , in keeping with the expected value of silver. Figure 3b shows the number of electrons as a function of impact energy in the last 20 ns of the simulation. Here, a clear peak is observed at  $\sim 700$  eV, with a significant number of impacts occurring for energies up to 2 keV.



**Figure 3 – a) Electron growth rate from CST Particle Studio, b) impact energies as a function of time, and c) as a function of emission phase.**

Using the 1-D particle tracker, and modelling the region of critical multipactor, the impact energy of an electron can be seen to depend on its emission from the helix, with respect to the phase of the RF signal. This is depicted in Figure 3c, where the electric field is assumed to vary as a sinusoid, and the electrons are emitted with an initial energy of 0.04 eV. Comparing the CST and 1-D results suggests that the high-energy electron impacts are those emitted from the helix at phase values between  $-2$  and  $100$  degrees. This would correspond to those electrons which see the largest acceleration from the RF field.

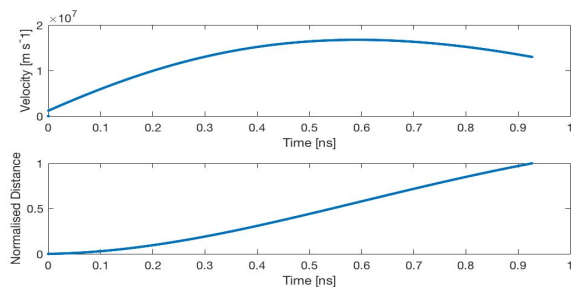


**Figure 4 – 1-D particle tracking results for an electron emitted from the helix, at an emission phase of 116 degrees.**

Figures 5 and 6 depict velocity and normalized distance (the ratio of the distance the particle has travelled and the gap between wall and helix) from the 1-D model, for emission from the helix and wall, respectively. Here, the electron has some initial energy, and is emitted at a phase of 116 degrees, with respect to the RF. On comparing the two, it can be seen the transit from wall to helix takes  $\sim 20\%$  longer, owing to the change in sign of the  $1/r$  electric field dependence experienced by the particle.

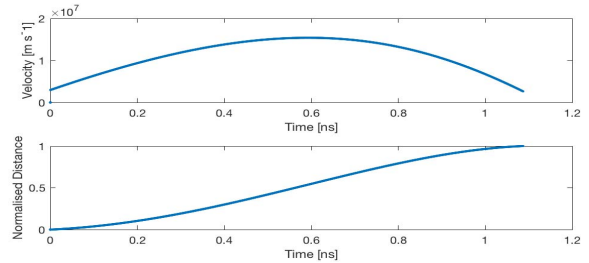


**Figure 6 – 1-D particle tracking results for an electron emitted from the wall, at an emission phase of 116 degrees.**

### III. SUMMARY

Particle-in-Cell and 1-D analytical calculations have been performed on a helical resonant filter geometry. A power study has been conducted, showing the effect of multipactor within the system. At a power level of 40 W, the average impact energy occurs at  $\sim 700$  eV. The 1-D model predicts that that electrons must be emitted at a phase of  $\sim 120$  degrees, with respect to the RF. Our current focus is on examining multi-carrier operation within the system, as well as refinement of the 1-D model.

### ACKNOWLEDGMENTS

This work has been funded by the STFC, research project ST/N00230X/1.

### REFERENCES

- [1] A. I. Zverev, Handbook of Filter Synthesis. New York: Wiley, 1967, ch. 9, pp. 499–521.
- [2] S. J. Fiedziuszko and R. S. Kwok, "Novel helical resonator filter structures," in IEEE MTT-S Int. Dig., 1998, pp. 1323–1326.
- [3] K. Clark and C. Thamviriyakul, "A Possible Explanation for the Brief Life-Span of UoSAT-4," in 11<sup>th</sup> Amsat-UK Conference, Surrey, UK.
- [4] J. R. M. Vaughan, "Multipactor," IEEE Transactions Electron Devices, VOL. 35, NO. 7, Pp. 1172–1180, July 1988.
- [5] A. Dexter and R. Seviour, "Rapid generation of multipactor charts by numerical solution of the phase equation," Journal of Physics D: Applied Physics, Vol. 38, No. 9, pp. 1383–1389, April 2005.
- [6] E. Doumanis, G. Goussetis, W. Steffe, D. Maiarelli, S.A. Kosmopoulos, "Helical Resonator Filters with Improved Power Handling Capabilities for Space Applications," IEEE Microwave and Wireless Components Letters, Vol. 20, No. 11, pp. 568–600, November 2010.
- [7] E. Lund, L. Bugge, I. Gavrilenko and A. Strandlie, "Track parameter propagation through the application of a new adaptive Runge-Kutta-Nystrom method in the ATLAS experiment," Journal of Instrumentation, Vol. 4, P04001, April 2009.